LRP 660/00 January 2000

Central electron temperature enhancements due to sawtooth stabilization during counter ECCD in TCV

Z.A. Pietrzyk, C. Angioni, R. Behn, S. Coda,
T.P. Goodman, F. Hofmann, M.A. Henderson,
J.-P. Hogge, J.-M. Moret, A. Pochelon,
H. Reimerdes, O. Sauter, H. Weisen

submitted for publication in
Physics of Plasma

ISSN 0458-5895

Central Electron Temperature Enhancements due to Sawtooth Stabilization during Counter ECCD in TCV

Z.A. Pietrzyk, C. Angioni, R. Behn, S. Coda, T.P. Goodman, F. Hofmann, M.A. Henderson, J-P.Hogge, J-M. Moret, A. Pochelon, H. Reimerdes, O. Sauter, H. Weisen

Centre de Recherches en Physique des Plasmas, Ecole Polytechnique Fédérale de Lausanne,

Association EURATOM-Confédération Suisse, CH-1015 Lausanne, Switzerland

Abstract

In the TCV tokamak, the central electron temperature obtained in discharges with counter (CNTR) electron cyclotron current drive (ECCD) is larger than with CO-ECCD or electron cyclotron resonance heating (ECRH) alone. Comparison of experimental results with calculations by the transport code PRETOR indicates that sawtooth stabilization is responsible for the increased confinement time and the attendant twofold enhancement of the central temperature. Sawtooth stabilization is caused in turn by the central safety factor q_0 rising above 1 for CNTR-ECCD; by contrast, the simulation results show that $q_0<1$ in the sawtoothing CO-ECCD and ECRH cases.

52.55.Fa,52.50.Gj,52.25.Fi

Introduction

Electron Cyclotron Resonance Heating (ECRH) provides very localized power deposition in the plasma owing to a narrow resonance absorption layer and a small beam cross section. In this paper we define ECRH as a case with the beam injection angle perpendicular to magnetic axis. Electron cyclotron waves influence the plasma current distribution in several ways. The temperature rise at the absorption location increases the local conductivity and electric current increases in that location, thus modifying the current profile. By adding a toroidal component to the wave vector of the launched EC waves, additional current is driven parallel (CO-ECCD) or anti-parallel (CNTR-ECCD) to the Ohmic current. In recent experiments in TCV, total replacement of the Ohmic current has been achieved by CO-ECCD[1] in quasi steady state discharges.

Central CNTR-ECCD, in combination with the Ohmic current, can produce a hollow current profile with negative magnetic shear in the plasma core, a situation known to be conducive to Internal Transport Barrier (ITB) formation [2]. In TCV it was previously observed that the sawtooth period can be modified by changing the power deposition location relative to the q=1 surface[3]; in particular, the maximum period is observed when power is deposited on or near the q=1 surface. In addition, even in the absence of a toroidal wave-vector component, the shape and period of the sawteeth are affected by the small ECCD component due to the pitch angle of the magnetic field lines on the q=1 surface; this effect is responsible for an up-down asymmetry in the heating location with respect to sawtooth behavior[4].

The T-10[5] and TCV[6] experiments previously reported higher central electron temperatures with CNTR-ECCD than with CO–ECCD or ECRH for the same plasma configurations. The earlier TCV results, obtained with 0.5 MW of EC power, were inconclusive, as the difference was only slightly larger than the error bars. In the present paper, we report on further investigation with 1.5 MW power and with a systematic scan of the toroidal injection angles to change the amount of driven current. The energy confinement time is found to increase with CNTR-ECCD. The central heat diffusivity drops to the Ohmic level, but not to the neoclassical level characteristic of ITBs[2]. Our results show that the improved performance in TCV can be fully explained by sawtooth stabilization, without invoking additional effects related to negative magnetic shear. Since sawtooth crashes eject energy from the plasma core, their elimination naturally results in a larger average central temperature. This effect had already been documented a decade ago in JET[7], where sawtooth-free periods of up to 1.6 s were observed during combined Neutral Beam Injection and Ion Cyclotron Heating, being terminated by crashes that caused a temperature drop of up to 50%.

The present experiments were performed on a weakly elongated (κ=1.2) plasma, which was moved vertically during each discharge, across the microwave beam, to study the influence of the ECCD deposition location on fast electron generation[8]; however, this aspect of the experiment will not be discussed here. The increased electron temperature described here was achieved only with CNTR-ECCD applied near the magnetic axis; even though sawtooth stabilization was observed in other heating and current-drive

scenarios, the energy deposited in the core was smaller in those cases and did not result in as high central temperatures.

Experimental setup

TCV is a medium-sized tokamak (R=0.88 m, a=0.25 m, Ip≤1MA)[9], equipped at the time of experiment with 3 gyrotrons of 0.5 MW each and a very flexible beam delivery system[10] which allows EC power deposition at any plasma location with or without a toroidal wave-vector component. This setup permits, in particular, a comparison of shots with CO- or CNTR-ECCD with shots without toroidal injection, with the same radial heating location. In addition, the TCV plasma control system permits a wide range of vertical plasma motion within the highly elongated (κ_v=3) vacuum vessel in the course of a shot[9], providing further options for changing the heating location. Diagnostics used in this study include a Thomson scattering system with 3 YAG lasers operating at a 20Hz repetition rate each, soft X-ray tomography, and magnetic probes.

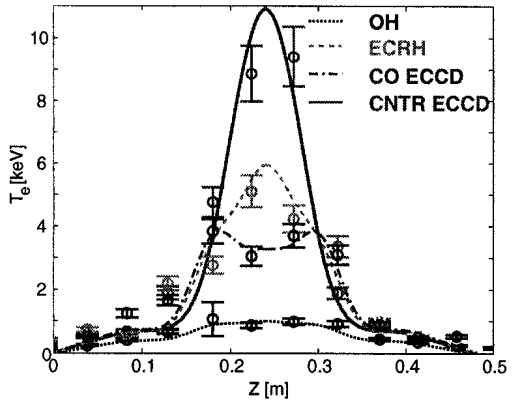

Figure 1. Electron temperature profiles with CNTR-(–28° toroidal injection angle), CO -ECCD (21° toroidal injection angle) and with ECRH. An Ohmic case is shown for reference. Centrally located power deposition.

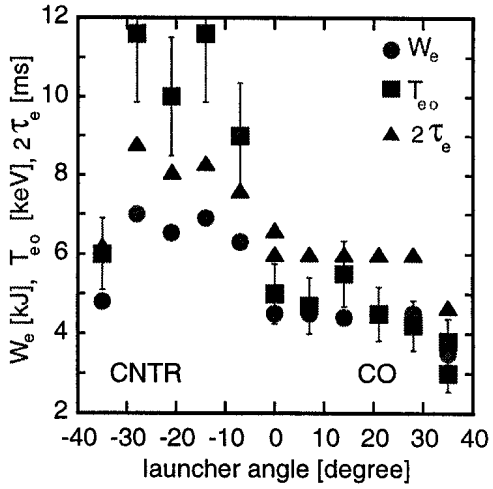

Figure 2. Plasma performance for different toroidal injection angles: total electron energy, central electron temperature and electron confinement times versus launching angle.

The plasma parameters were as follows: κ=1.2, δ=0.2, q_a=5.5, $n_{eo}=2.10^{19}m^{-3}$, I_p=170kA. The full 1.5 MW EC power was deposited in a central location (ρ = 0-0.1 and $\Delta\rho$=0.1) at the beginning and at the end of each discharge, and at an off-axis location near the q=1 surface (ρ=0.25) in the middle part of the discharge (t=0.7-1.25s). In this paper the normalized radius ρ is a flux coordinate defined as the square root of the ratio of the volume enclosed by a given magnetic flux (ψ) surface to the total plasma volume, $\rho(\psi) \equiv \sqrt{\frac{V_\psi}{V_{edge}}}$. The ECCD efficiency depends strongly on the toroidal injection angle and has been found to be greatest with an angle of 35° [8]. By contrast, the amount of energy deposited in the plasma is essentially independent of the angle, if the beam is fully absorbed during the first pass. A systematic scan of the angle was carried out in the experiments described.

Experimental results

Typical electron temperature profiles are shown in Fig. 1 for the CNTR-ECCD, CO-ECCD, ECRH and Ohmic cases for comparison. The central temperature is approximately twice as high in the CNTR-ECCD case than in the other EC-heated discharges with equal power. No sawteeth are observed during central CNTR-ECCD. It should be noted that the difference between the CO-ECCD and ECRH cases, in which sawteeth are present, is not significant, as it is smaller than the variation during a single sawtooth.

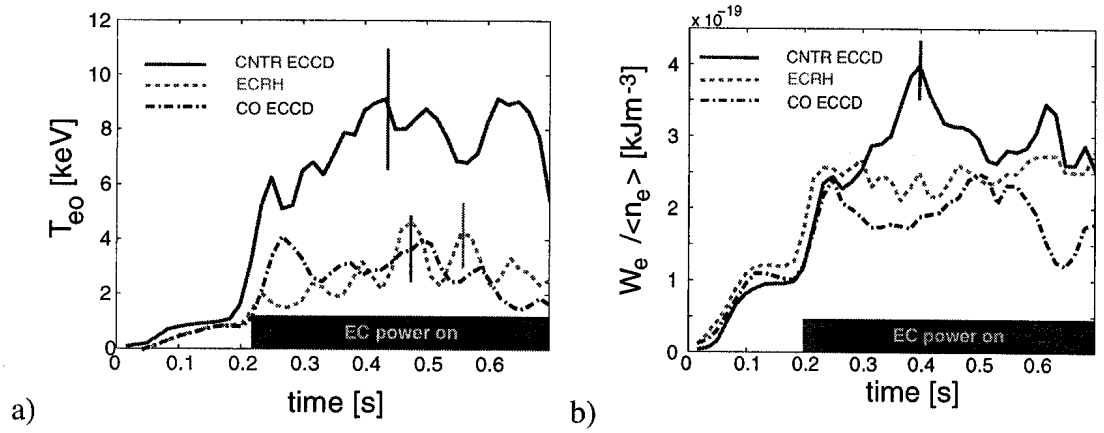

Figure 3. Evolution of: a) Central electron temperature, b) total electron energy normalized to the volume average density, as functions of time, for shots with CNTR- and CO-ECCD and ECRH.

A strong dependence of plasma performance on the direction and magnitude of the central driven current is found by a systematic variation of the toroidal injection angle. This is clear in Fig. 2, which shows the total electron energy, the largest value of the central electron temperature and the electron energy confinement time as functions of the injection angle (here, negative angles corresponds to CNTR-ECCD). Angles that are larger in absolute value have larger current-drive efficiencies[8]. All the quantities shown reach a maximum in the region between -14 and –28°. The drop observed at the highest angles, both positive and negative, is probably caused both by a displacement of the absorption layer away from the magnetic axis, induced by fast-electron Doppler shift, and by an increased beam size due to the beam refraction. Calculations by the ray tracing code TORAY[11] show that the power is always deposited inside the q=1 surface, except at the 35° angle, at which the power is deposited at the q=1 surface. The time evolution of the central temperature and of the total electron energy normalized to the volume-averaged density is shown in Fig. 3. This confirms the enhanced performance of CNTR-ECCD discharges.

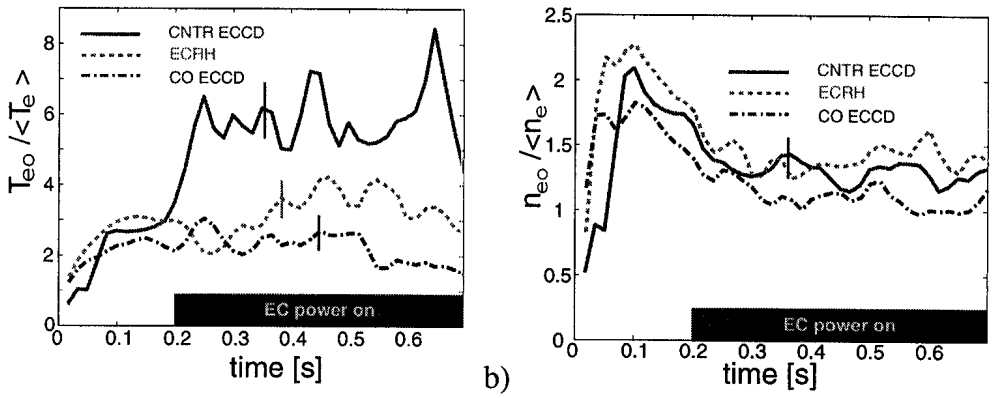

Figure 4. Peaking factors of a) temperature $\frac{T_{eo}}{<T_e>}$ *and b) density* $\frac{n_{eo}}{<n_e>}$ *, versus time for shots with CNTR- and CO-ECCD and with ECRH.*

As a measure of core confinement, it is especially instructive to study the behavior of the peaking factors for both temperature and density. As shown in Fig. 4, the temperature profile is considerably more peaked in the CNTR-ECCD case than in the CO-ECCD and ECRH cases, whereas the density profile is essentially the same in all three types of discharge. This indicates that the thermal losses from the plasma center are reduced during CNTR-ECCD, while particle transport is unchanged.

An effective heat transfer coefficient can be defined as $\chi_e \equiv -\frac{Q_e}{n_e \nabla T_e}$, where Q_e is total power density. Figure 5 shows the radial variation of χ_e for typical discharges with CNTR-ECCD, CO-ECCD, ECRH and Ohmic heating alone calculated from smoothed experimental data. It is found that near the plasma center the heat transfer coefficient for CNTR-ECCD is about four times lower than for CO-ECCD and ECRH, and is almost as low as in the Ohmic case (although the latter is still one order of magnitude higher than the neoclassical value). Therefore, the confinement degradation due to the additional heating power is almost completely eliminated for $\rho<0.4$ during CNTR-ECCD. The

improvement in global confinement is less pronounced, as the confinement remains degraded in the region $\rho>0.4$. The local maximum observed in χ_e for $\rho\sim0.55$ is due to a flattening of the temperature profiles at this location, which may be caused by mode activity as suggested by often observed the up-down asymmetries in the raw Thomson temperature profiles.

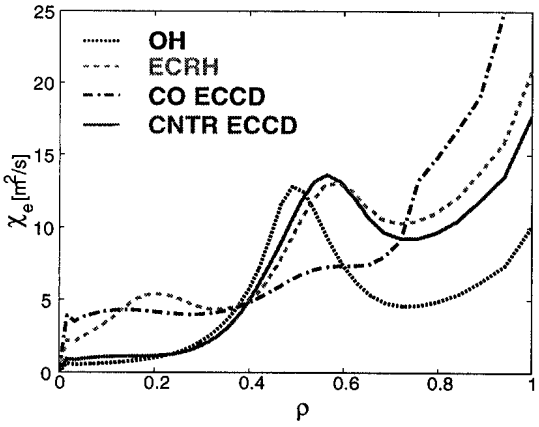

Figure 5. Effective heat transfer coefficient for shots with CNTR-, CO-ECCD, ECRH and Ohmic heating only.

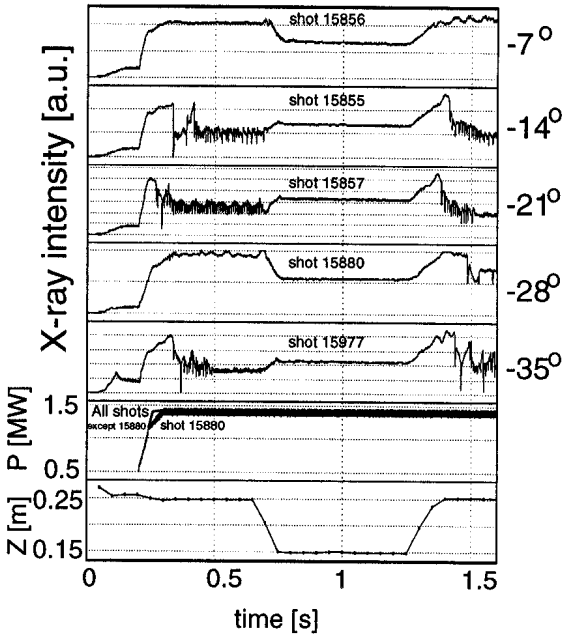

Figure 6. Soft X-ray traces from a vertical X-ray camera for CNTR-ECCD shots with different toroidal injection angles. The traces of EC power P and plasma positions Z is common to all shots (except shot 15880 with different form of power increase). Most shots show rapid degradation of plasma performance; only two discharges (15856 with -7° injection angle and 15880 with -28° injection angle) show long quasi-stationary phases.

The high-performance phase of CNTR-ECCD discharges can last longer than the time for the current profile to relax, and is often terminated by a catastrophic event accompanied by sudden energy loss. This is reflected in a sudden drop in the soft X-ray emissivity, as shown in Fig. 6 for a signal from a vertical-looking camera, for different toroidal injection angles. As the angle increases, the current drive efficiency increases while the

EC beam becomes larger and the absorption layer moves outward. The collapse of the X-ray signal is seen in all discharges, with the exception of the –7° case and of the first of the two central-heating phases in the –28° case. We can speculate that the good behavior of the –7° case is due to the driven current being small. In the –28° case, the only apparent difference between the early quiet central-heating phase and the later one, which results in a collapse, is the slower power ramp-up of the former.

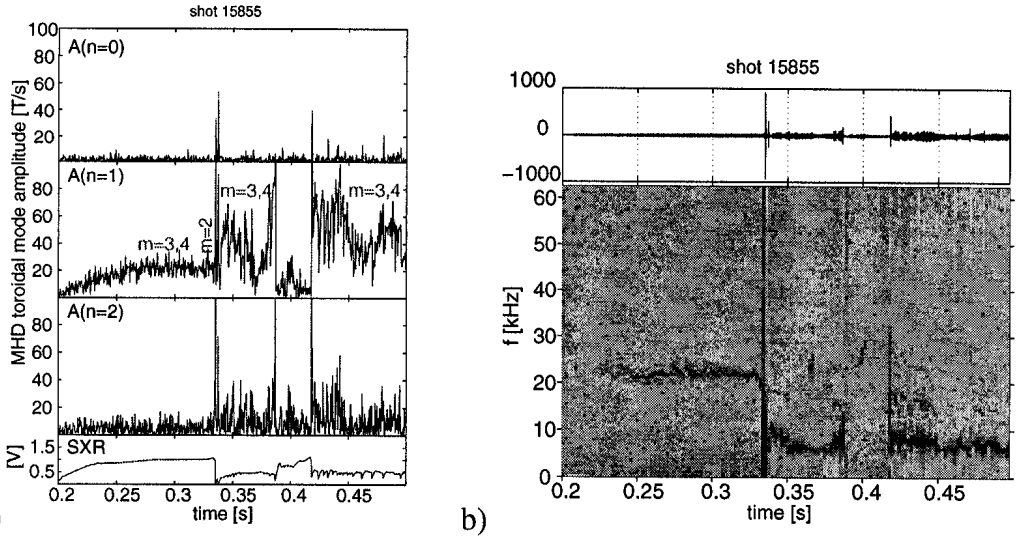

Figure 7. Magnetic mode analyses a) different toroidal mode- number component with an indication of corresponding poloidal numbers. b) Fourier analysis for the same shot. Safety factor q_a=5.5.

Analysis of fast magnetic probe data has been performed with a view to elucidating the dynamics of the collapse, see Fig. 7. A mode with toroidal and poloidal numbers n=1, m=3 and 4, and with a frequency of 20 kHz, is present in all high-performance phases, when T_{e0} > 5keV. After the X-ray signal crash this mode slows down to about 7 kHz, the typical frequency for ECRH discharges. At the present stage the role of this mode is not completely understood. However, one can see from the Fig. 7 that the high frequency mode exists during the high soft X-ray intensity phase.

Simulations by the PRETOR transport code

The transport code PRETOR[12] was used to assist in the interpretation of the results. The code includes sawtooth triggering criteria and can thus be used to investigate plasma behavior in sawtoothing discharges. The transport coefficients were taken from the RLW model[13]. The plasma density profiles measured by Thomson scattering, cross calibrated to interferometer data, were used in the calculation. The power deposition location, the absorption width and the amount of driven current, all of which must be given to PRETOR in input, were obtained from the ray tracing code TORAY [11]. PRETOR itself calculates the bootstrap current fraction.

Representative temperature and safety-factor profiles generated by PRETOR are shown in Fig. 8. The difference between the CNTR-ECCD, CO-ECCD, ECRH and Ohmic temperature profiles is well reproduced. In order to assess the role of sawteeth in plasma performance, the CO-ECCD and ECRH cases were simulated again with an artificially increased sawtoothing threshold, thus simulating a sawtooth-free scenario: in this case the same result was obtained as with CNTR-ECCD. Hence these simulations support the assumption that the improved confinement in CNTR-ECCD discharges is due to sawtooth stabilization. The cause for this stabilization, suggested by Fig. 8b, is the central safety factor rising above 1. Since regions of negative or flat magnetic shear are predicted by the code to exist in all EC-heated cases, negative central shear does not appear to be a significant factor in the enhanced confinement.

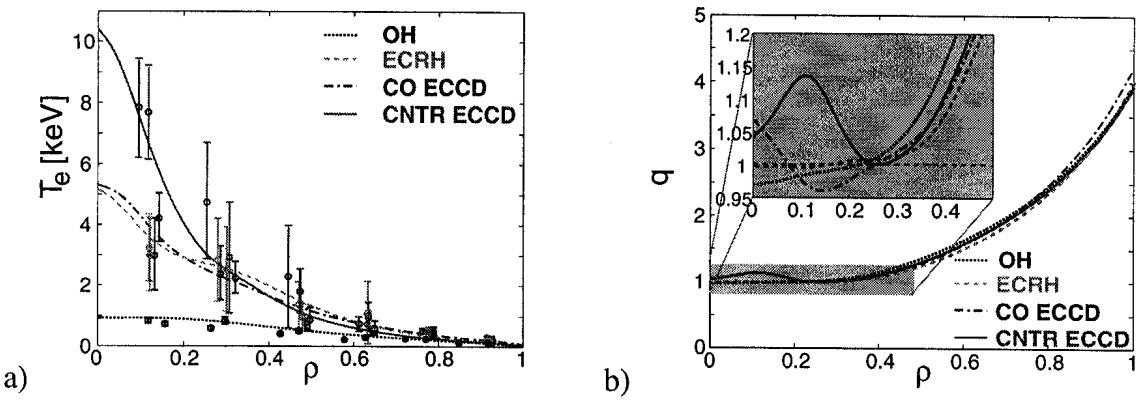

Figure 8. PRETOR transport code calculation results together with the experimental points a) temperature profiles, b) q profiles. Power deposition location (ρ=0.1) and beam width ($\Delta\rho$=0.1) taken from TORAY ray tracing code.

PRETOR also reproduces the temperature drop for the highest toroidal injection angle, -35°. This is due to the EC beam being broader and being shifted to the outer plasma region, where current-drive efficiency is lower.

Conclusions

Improved central energy confinement with a twofold increase of the central electron temperature and the formation of a steep core temperature gradient has been observed in TCV with CNTR-ECCD deposited near the magnetic axis. The central heat transfer coefficient decreases by a factor of 4 and the global electron energy confinement time increases by approximately 40% in these discharges compared with plasmas with ECRH alone or CO-ECCD.

Unlike thermal transport, particle transport does not vary appreciably from ECRH and CO-ECCD to CNTR-ECCD: while the temperature profile peaks significantly in the

CNTR-ECCD case, the density profile remains the same. The high-performance phase can last for more than the time for the current profile to relax; it is accompanied by a high-frequency (20 kHz) MHD mode and is usually terminated by a sudden collapse with the mode slowing down to about 7 kHz.

Calculations by the PRETOR transport code suggest that this improved confinement could be do to sawtooth stabilization induced by the central safety factor q_0 rising above 1; by contrast, PRETOR predicts $q_0<1$ for CO-ECCD and ECRH discharges. This result is in good agreement with experiment, as sawteeth are present in discharges with central CO-ECCD or ECRH but not with CNT-ECCD. The poorer central confinement observed in sawtoothing discharges is due to the periodic core energy loss caused by sawtooth crashes.

Acknowledgements

The authors wish to thank to all TCV team for their help in this study. This work was partially supported by Swiss National Science Fund.

References

[1] O. Sauter, M.A. Henderson, F. Hofmann et al., "Steady-state non inductive scenario using electron cyclotron waves in a magnetically confined plasma" accepted to Phys. Rev. Letters (2000).

[2] L.L. Lao, K.H. Burrell, T.S. Casper et al., Phys. Plasmas **3**, 1951 (1996)., C.M. Greenfield, D.P. Schissel, B.W. Stallard et al., Phys. Plasma **4**, 1596 (1997)

[3] Z.A. Pietrzyk, A. Pochelon, T.P. Goodman et al., Nuclear Fusion **39,** 587 (1999).

[4] T.P. Goodman, M.A. Henderson, J-Ph. Hogge et al., Proc. 26th EPS Conf., Europhys. Conf. Maastricht, Abstracts 23J,1101 (1999).

[5] V.V. Alikaev, A.A. Badgdasarov, A.A. Borshegovskij, et al. Nuclear Fusion **35,** 369 (1995).

[6] T. P. Goodman, M.A. Henderson, F. Perthuisot, et al. Radio Frequency and Current Drive of Fusion Devices Brussels, 245 (1998).

[7] D.J. Campbell, D.F.H. Start, J.A. Wesson, et al., Phys. Rev Letters **60,** 2148 (1988).

[8] S. Coda, Y. Peysson, L. Delpech et al., Proc. 26th EPS Conf., Europhys. Conf. Maastricht Abstracts 23J,1097 (1999).

[9] F. Hofmann, J.B. Lister, M. Anton et al., Plasma Phys. Control Fusion **36,** B277 (1994).

[10] T.P. Goodman, S. Alberti, M.A. Henderson, A. Pochelon, M.Q. Tran Fusion Technology (Proc. 19th Symp. Lisbon 1996), Vol. 1, Elsevier, Amsterdam and New York 565 (1997).

[11] A.H. Kritz, H. Hsuan, R.C. Goldfinger, D.B. Batchelor, Heating in Toroidal Plasmas (Proc. 3rd Varenna-Grenoble Int. Symp., Grenoble, 1982), **Vol. 2**, CEC, Brussels 707 (1982).

[12] D. Boucher and P.H. Rebut, in Proc. IAEA Tech. Conf. on Advances in Simulation and Models of Thermonuclear Plasmas. Montreal 142 (1992), C. Angioni, D. Boucher, J.-M. Moret and O. Sauter, Theory of Fusion Plasmas Editrice Compositori Bologna 493 (1998).

[13] P.H. Rebut, P.P. Lallia, and M.L. Watkins, proc. 12th Int. Conf. Plasma Physics and Controlled Nuclear Fusion Research, Nice 1988 IAEA Vienna **I2**, 191 (1989).